This paper not to be cited without prior reference to the author

International Council for the Exploration of the Sea

C. M. 1980/C : 20
Hydrography Committee

THÜNEN
Digitalization sponsored by Thünen-Institut

# Variations of the current system in the Equatorial Atlantic at 28°40'W during FATE in May - June 1979

by

H. U. Lass, W. Fennel
R. Helm, M. Sturm

Academy of Sciences of the GDR
Institute of Marine Research
Rostock-Warnemünde
German Democratic Republic

## Abstract

The transient from typical northern winter to summer conditions in the equatorial circulation of the Atlantic ocean occured at 28° 40' W within the FGCE year during May to mid of June simultaneously with a transient of the meridional distribution of the zonal wind component from typical winter to summer conditions. Exceptional high values of the eastward component of the current core velocity (130 cm/s) and the mass transport (28 Sverdrup) of the Atlantic Equatorial undercurrent occured during the first half of May.

Obviously in response to a puls-like intensification of the SE Trades on 20th May 1979 variations with a time scale of about 10 days and with an amplitude comparable to the annual cycle were observed to occur in both the zonal circulation and the vertical exchange processes of the EUC. Simultaneously wave like processes at the equator could be observed.

## Introduction

As part of the FGGE Atlantic Tropical Experiment in 1979 oceanographic measurements were made from the RV "A. v. Humboldt" of the Institute of Marine Research of the Academy of Sciences of the German Democratic Republic along 28°40'W and 2°S to 6°N between 26th April and 17th June 1979.

Four surface moorings were deployed at 6°N, 4°N, 1°20'N and at the equator between 27th and 29th April. The moorings at 1°20'N, 4°N and 6°N were recovered during 13th to 17th June. The equator mooring was lost after 1st June likely by electrolytic corrosion. The moorings at 1°20'N and at 4°N supplied useful time series of current measurements at 15 m and 70 m depth respectively at 15 m, 70 m, 90 m and 175 m depth. All the other instruments had malfunctions.

Eight sections were occupied during 8th May to 2nd June and a further section was made between 13th and 17th June (Fig.1). A total of 70 stations were completed along the sections consisting of 45 CTD current-profiler lowerings to at least 600 m depth and 25 Nansen casts and current-profiler lowerings to at least 200 m depth. At 66 stations profiles of temperature, conductivity, oxygen, sound velocity, phosphate and the meridional and the zonal component of the current vector were measured.

At each station corresponding measurements of hydrostatic pressure, temperature, salinity, oxygen and current were made at a single depth for comparison with the profile measurements.

From those comparison measurements regression curves for the systematic errors of the sensors have been estimated for the pressure, temperature, conductivity sensor and the current measurements. The remaining standard deviations between the corrected measurements of the CTD and the bottle samples were



1.5 m, 0,01°C and 0,01 °/oo for the first 25 stations, 0,02 °/oo for the remaining 20 stations and all along 10cm/s for the current measurements.

The comparison between oxygen sensor and bottle measurements showed that the sensor had malfunctions due to the diffusion membrane. So the bottle measurements were used only.

All measurements of the CTD were subject of a validation routine which eliminated too large spikes and steps in the original measurements, made the static corrections, eliminated all scans which were influenced by eddies penetrating the sensors by means of the Rosette-bottles due to ships motions and calculated mean values for standard levels.

No dynamical error due to response lag of the temperature sensor was found obviously because the time lag of the sensors was shorter than the 1 second integration in each scan. Deviations from classical TS diagramms of the Equalant I, II expeditions below the 12°C isotherm were subject to a further static correcture.

The measurements were made in order to study the variability of the Equatorial Undercurrent, the South Equatorial Current and the North Equatorial Counter Current in time and meridional direction in a transient stage from boreal winter to summer conditions.

## Results

### Windfield

The position of the ITCZ was derived from the change of the sign of the meridional wind component. Fig. 2 shows the ITCZ to be in its mean position during May to June 1979 near 30°W. Visual observations showed oscillations of the ITCZ around its mean position with periods of some days.

Fig. 3 shows that the meridional distribution of the zonal windstress is typical for winter conditions at 8th to 12th May and typical for summer conditions one month later.

The time series of the mean of the windstress between 2°S and 2°N in Fig. 4 a, b depicts this region to be under the action of the SE Trades which are generally weaker than the long time mean in May - June except a strong pulse around 20th May. The time series of the meridional wind component shows fluctuations with a period around 6 days in May - June (Fig. 5). In comparison with the meridional distribution of the dynamic depth anomaly during Equalant I and II at 25°W (Fig. 6), the distribution during FATE at 28°40'W (Fig. 7) indicates typical winter conditions during 8th to 12th May and typical summer conditions during 12th to 17th June with a high pressure ridge at 4°N however not so strong developed as during Equalant II.

The meridional distribution of zonal current component between 2°S and 6°N at 28°40'W during 8th to 12th May and 12th to 17th June (Fig. 8) suggests also a transient from winter to summer conditions, because during 12th to 17th June there is a well developed SEC between the equator and 4°N and northward of 4°N the NECC could be observed.



From the observations of the meridional wind, dynamic depth anomaly and zonal current velocity we conclude that the transient from typical northern hemisphere winter conditions to typical summer conditions occured at the equator at 28° 40'W during nearly one month from 10th May to 15th June 1979.

### Meridional sections

The depicted meridional sections of the zonal current in Fig. 9 and 10 show a well developed Equatorial Undercurrent at 28°40'W with high velocities in the core ranging between 88 cm/s and 131 cm/s in a depth range from 80 m to 50 m. The meridional extent of the undercurrent is roughly between 1,5°S and 1,5°N. After the intensification of the zonal windstress on 20th May the core of the EUC shifts southward to 0,5° - 0,75°S crossing the equator again on 31st May. In most cases the EUC reaches the surface although the surface winds are directed westward. Obviously this current pattern causes the extremely high zonal transport of the EUC before 20th May which is twice as high as known from GATE at nearly the same position (Table 1).

It is surprising that such high transports and velocities are to be measured in the core of the EUC during a time of low zonal pressure gradient (after KATZ and Collaborators 1977). A comparison of the "A. v. Humboldt" measurements with historical measurements of the EUC core velocities near 30°W is shown in Fig. 11 and indicates a maximum in the yearly variations of the core velocity at the time of a rising zonal pressure gradient after the yearly minimum. This suggests a phase lag between the driving zonal pressure gradient, which is the response of the equatorial zone to the wind over the entire equatorial wave guide, and the dissipating forces of the EUC which could depend on the wind over the smaller meridional belt of the EUC width only.

The current pattern below the EUC is highly variable in time. We could not measure a persistent westward directed counter current at 28°40'W between 8th May and 17th June.

During 17th to 19th May the South Equatorial Current is developing north of the EUC at a depth of about 90 m and remains at this depth to the end of May, indicating that baroclinic processes play an important part in the generation of this current north of the equator.

Meridional sections of temperature and phosphate are shown in Figs. 12 and 13. They show throughing below the EUC together with high temperatures and low phosphate contents in the surface layer before the 20th May only indicating a low vertical exchange typical for the winter situation.

The sections after the 20th May show as well throughing below as ridging above the EUC core with lower temperatures and high phosphate content in the surface layer. The latter underlines the part of the equator as an upwelling region. This patterns are typical for the summer conditions with intense vertical exchange processes.

Temporal variations of the Atlantic Equatorial Undercurrent

Table 1 shows that the EUC responds very quickly and intensely to a pulse-like intensification of the SE Trades. As well the meridionally averaged zonal component of the surface velocity as the zonal component of the core velocity and the eastward directed transport of the EUC are weakened within roughly 5 days after the onset of the SE Trades pulse. The eastward transport is lowered drastically to an amount of 50 % of the values before the onset of the SE Trades pulse. The variations of the transport within the 20 cm/s isotache could be beared by the fact that this isotache is leaving the area of observation during the meridional excursions of



the EUC. However the transport within the 40 cm/s isotache showed the same amount in its variations although this isotache did not leave the area bounded by 2°S and 2°N. Therefore we can conclude that both the eastward core velocity and the eastward transport of the EUC show variations of the magnitude of the yearly cycle already within a time scale of the order of 10 days.

The inspections of the meridional time plot of the salinity of the EUC and the zonal component of velocity shown in Figs. 14 and 15 indicate that the variations of velocity and transport are accompanied by a meandering of the EUC similar to that observed by DÜING et al. (1975) during GATE. Moreover not only the zonal component of the velocity field but also the vertical transport processes of the Atlantic EUC respond within a time scale of the order of ten days as indicated by the meridional distribution of temperature and phosphate before and after the onset of the SE Trades intensification as shown in Figs. 12 and 13. This observation is underlinded by the meridional time plot of the surface salinity (Fig. 14) which shows an enrichment of salinity above the EUC core after the 20th May suggesting an intensification of the vertical exchange processes.

References

DÜING, W., PH. HISARD, E. KATZ, J. MEINCKE, L. MILLER, K.V. MOROSHKIN, G. PHILANDER, A.A. RYBNIKOV, K. VOIGT and R. WEISBERG, 1975:
Meanders and long waves in the equatorial Atlantic. NATURE, 257, 280-284

KATZ, E. J. and Collaborators, 1977: Zonal Pressure Gradient along the Equatorial Atlantic. J. Mar. Res. 35, pp. 293-307

SCHEMAINDA, R., W. KAISER, D. NEHRING und S. SCHULZ, 1976:
Ozeanologische Untersuchungen im tropischen Nordatlantik auf 30°W zwischen 2°N und 15°N. Geodät. und Geophys. Veröff., R. IV, 17, 56 S.

Figure Captions

Fig. 1 Time-latitude diagram of oceanographic work by RV "A. v. Humboldt" during SOP II (May 8 - June 17 1979). Black circles represent oceanographic stations sampled by the electronic measuring system OM 75 and the profiling current meter WPS I along 28°40'W. Open circles indicate oceanographic stations sampled by Nansen bottles, reversing thermometers and the profiling current meter WPS II. Black squares $B_1$ - $B_4$ indicate current meter moorings along 28°40'W. Black triangles $B_1$ - $B_3$ represent recover ($B_2$ - $B_3$) respectively partial recover ($B_1$) of the current meter moorings. Open triangle is the position of the total loss of current meter mooring $B_4$. Black rectangles represent the installation and recover of a selfrecording wind measuring system on St. Peter and Paul Rocks. Double circles with cross indicate rendezvous with RV "Victor Bugaev" at 29°W for oceanographic and meteorological intercomparisons.

Fig. 2 Yearly cycle of positions of the area of the NE and SE Trades and ITCZ at 30°W after SCHEMAINDA et al., 1976. Positions of the ITCZ at the beginning and the end of the expedition of RV "A. v. Humboldt" at 28°40'W are indicated by bars.

Fig. 3 Meridional distribution of the meridional velocity component of wind (a) and the zonal component of wind stress (b) along 28°40'W at the beginning (x) and at the end (o) of the observing period.



Fig. 4 Mean values (dots) and deviations (bars) of the zonal (a) and meridional (b) wind stress averaged between 2°S and 2°N at all sections along 28°40'W occupied by RV "A. v. Humboldt" during FATE.

Fig. 5 Time series of the meridional component of wind velocity estimated from standard meteorological surface observations on board RV "A. v. Humdoldt" along 28°40'W and between 2°S and 2°N.

Fig. 6 Meridional distribution of the dynamic depth anomaly along 25°W measured during Equalant I by RV "Crawford" and during Equalant II by RV "Casco".

Fig. 7 Meridional distribution of the dynamic depth anomaly along 28°40'W measured by RV "A. v. Humboldt" during 8th to 12th May and 12th to 17th June 1979.

Fig. 8 Meridional sections of the zonal velocity component of current along 28°40'W and between 2°S and 6°N early in SOP II (8 - 12 May 1979) and at the end of SOP II (12 - 17 June 1979).

Figs. 9, 10 Consecutive meridional sections of the zonal velocity component of current along 28°40'W and between 2°S and 2°N during the main observing period (May 8 - June 2 1979).

Fig. 11 Yearly variations of the zonal component of current within the EUC core near 30°W from different expeditions independent of the year of observation.

Fig. 12 Meridional sections of temperature along 28°40'W before (14 - 16 May) and after (23 - 25 May) the intensification of the SE Trades.

Fig. 13 Meridional sections of phosphate along 28°40'W before (14 - 16 May) and after (29 - 30 May) the intensification of the SE Trades.

Fig. 14 Time-latitude diagram of salinity at 10 m depth along 28°40'W between 2°S and 2°N during SOP II (8 May - 2 June 1979).

Fig. 15 Time-latitude diagram of the zonal velocity component of current within the undercurrent core along 28°40'W and between 2°S and 2°N during SOP II (8 May - 2 June 1979).

T A B L E 1

Features of the EUC at 28°40'W during the FATE 1979 measured by RV "A.v.Humboldt"

| D | 8.-10.5. | 14.-16.5. | 17.-19.5. | 20.-22.5. | 23.-25.5. | 26.-27.5. | 28.-31.5. | 1.-2.6. | 12.-17.6. |
|---|---|---|---|---|---|---|---|---|---|
| $-\bar{\tau}_x$ [dyn/cm²] | ± 0.03 0.07 | ± 0.31 0.18 | ± 0.33 0.11 | ± 0.59 0.16 | ± 0.08 0.12 | ± 0.46 0.31 | ± 0.44 0.12 | ± 0.42 0.23 | ± 0.18 0.18 |
| $\bar{u}_{10}$ [cm/s] | ± 23 22 | ± 12 15 | ± 12 14 | ± 3 11 | - 20 ± 12 | ± 0 12 | - 22 ± 33 | ± 2 15 | ± 0 25 |
| $u_c$ [cm/s] | ± 117 10 | ± 131 10 | ± 103 10 | ± 117 10 | ± 88 10 | ± 124 10 | ± 120 10 | ± 126 10 | ± 112 10 |
| $d_{uc}$ [m] | 70 | 70 | 51 | 60 | 50 | 70 | 63 | 69 | 80 |
| $T_x$ [$10^6 m^3/s$] | ± 28 6 | ± 28 6 | ± 26 6 | ± 26 6 | ± 14 3 | ± - - | ± 20 5 | ± - - | ± 19 4 |
| $\overline{\Delta D}$ [dyn m] 10/500 db | 0.880 ± 0.007 | 0.882 ± 0.004 | 0.859 ± 0.003 | 0.870 ± 0.007 | 0.850 ± 0.008 | 0.857 ± 0.002 | 0.841 ± 0.011 | 0.870 ± 0.013 | 0.857 ± 0.008 |

The meridional mean values of eastward component of wind stress is denoted by $\bar{\tau}_x$, the eastward component of current at the 10 db level by $\bar{u}_{10}$ and the dynamic depth anomaly in the 10/500 db level by $\overline{\Delta D}$. The eastward component of current velocity in the EUC core is denoted by $u_c$, the depth of the EUC core by $d_{uc}$ and the eastward component of the volume transport within the 20 cm/s isotache by $T_x$. Averages are taken between 2°S and 2°N.

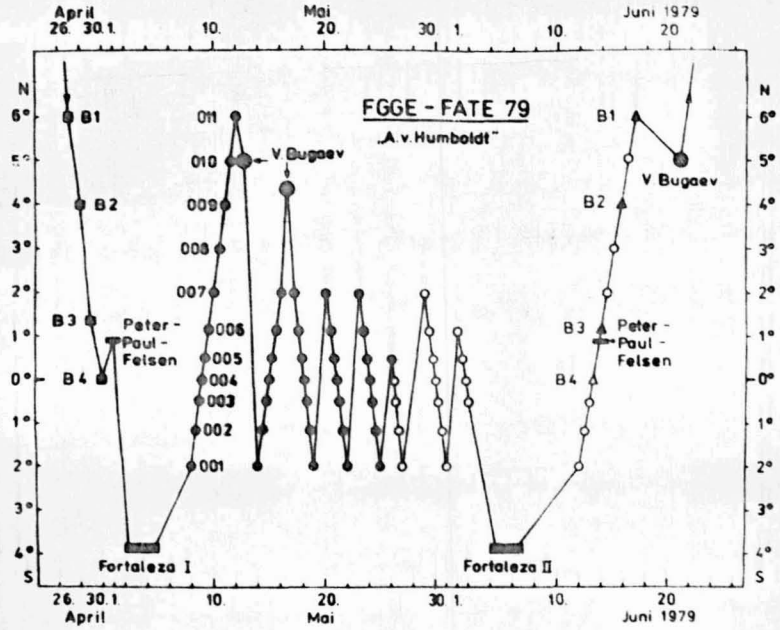


Abbildung 1

Fig. 1

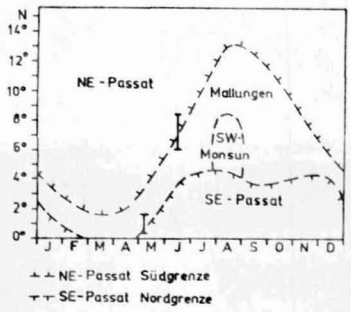


Fig. 2

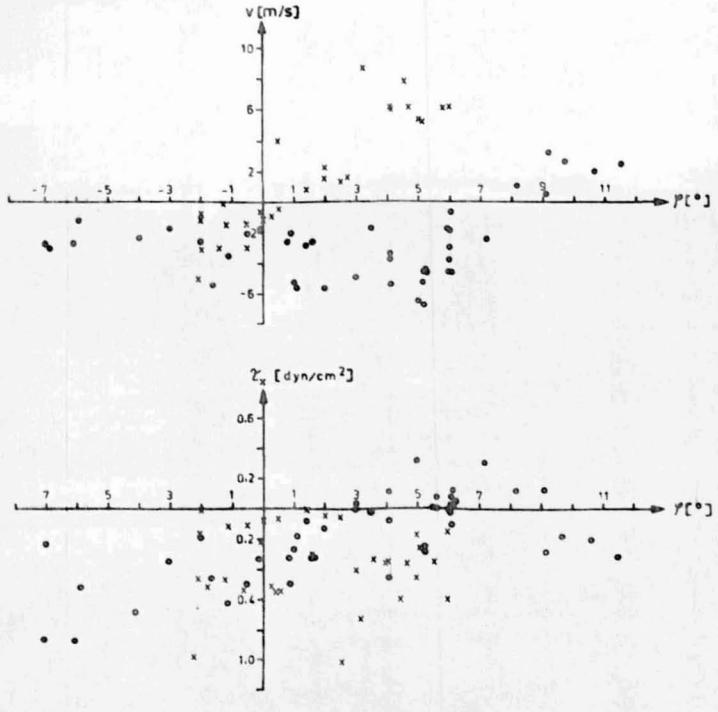


Fig. 3

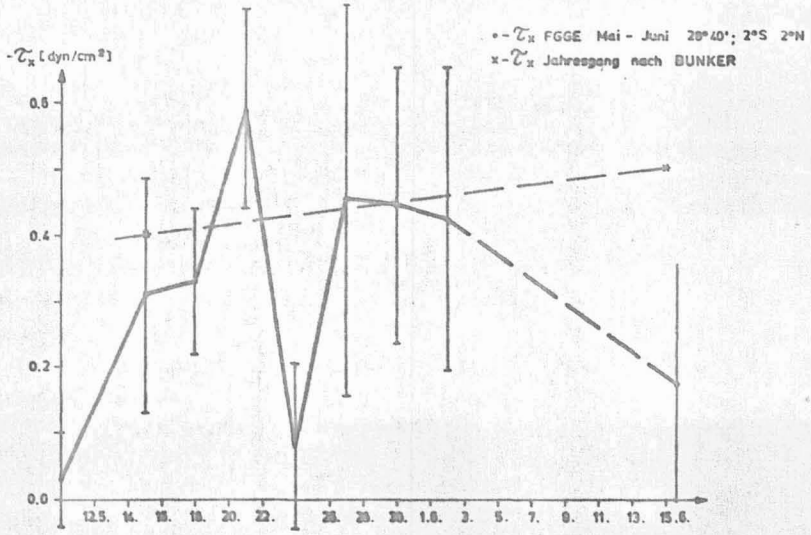


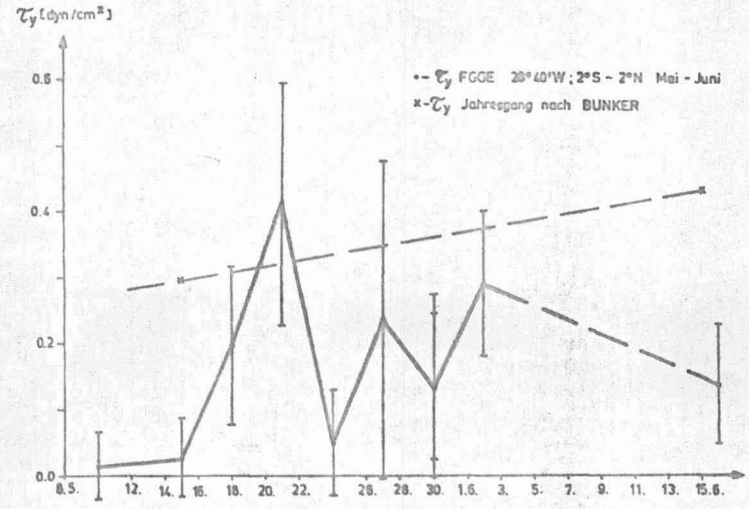


Fig. 4

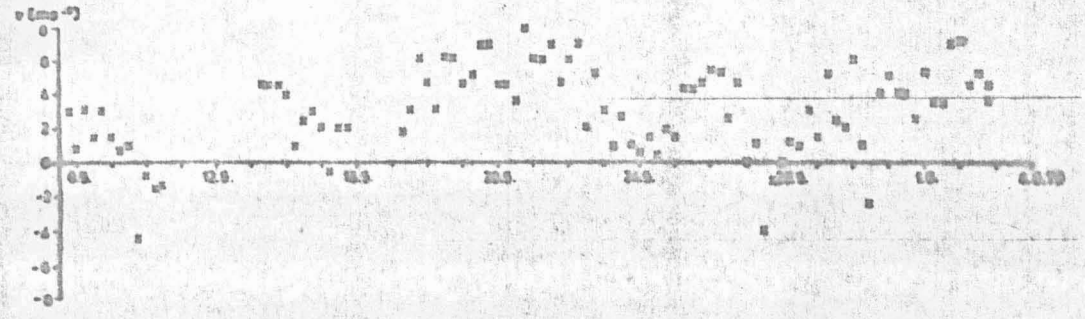

Abbildung 15

Fig. 5

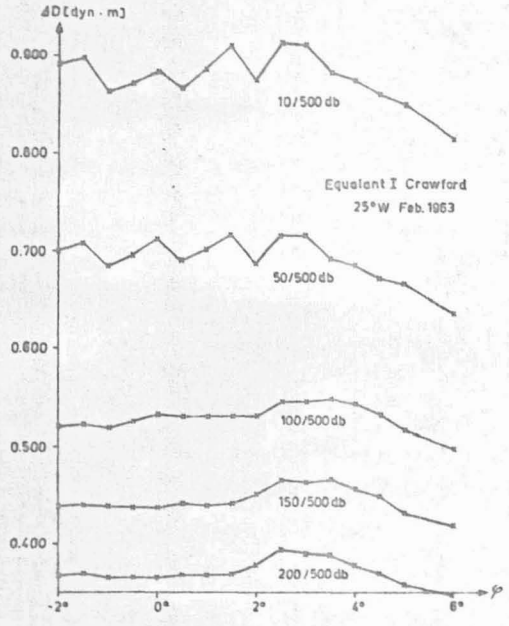
ΔD [dyn · m]
0.900
0.800
0.700
0.600
0.500
0.400
10/500 db
Equalant I Crawford
25°W Feb. 1963
50/500 db
100/500 db
150/500 db
200/500 db
-2°
0°
2°
4°
6°
φ

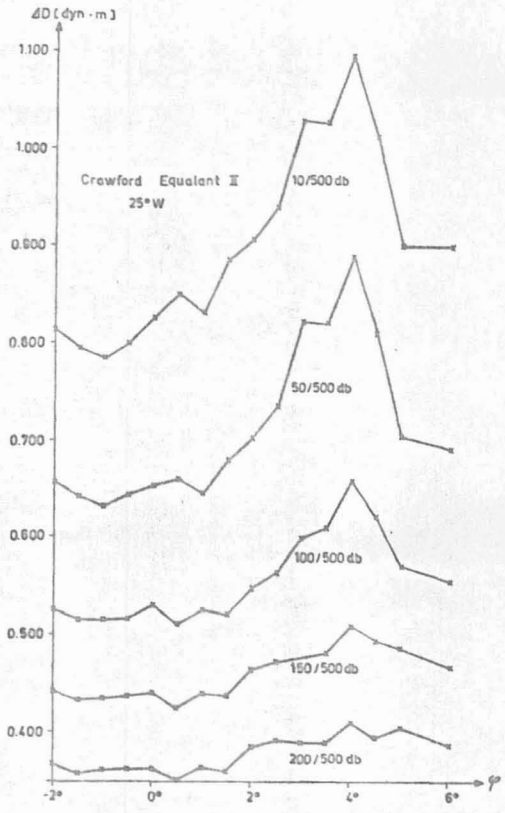
ΔD [dyn · m]
1.100
1.000
0.900
0.800
0.700
0.600
0.500
0.400
Crawford Equalant II
25°W
10/500 db
50/500 db
100/500 db
150/500 db
200/500 db
-2°
0°
2°
4°
6°
φ

Fig. 6

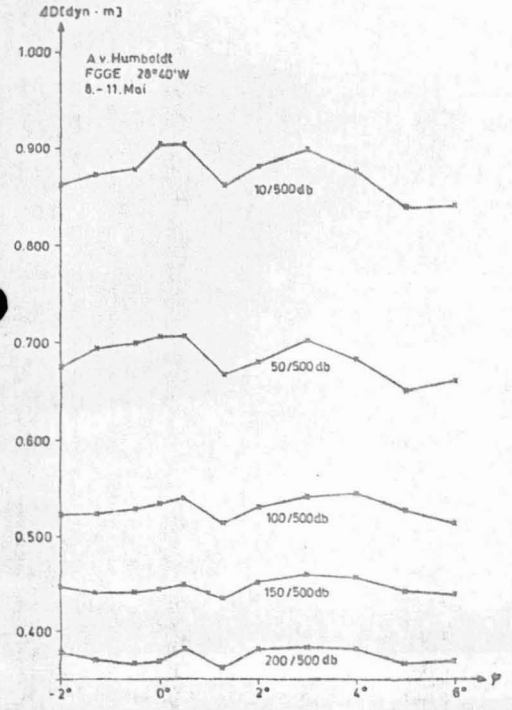
ΔD [dyn · m]
1.000
0.900
0.800
0.700
0.600
0.500
0.400
A v. Humboldt
FGGE 28°40'W
8. - 11. Mai
10/500 db
50/500 db
100/500 db
150/500 db
200/500 db
-2°
0°
2°
4°
6°
φ

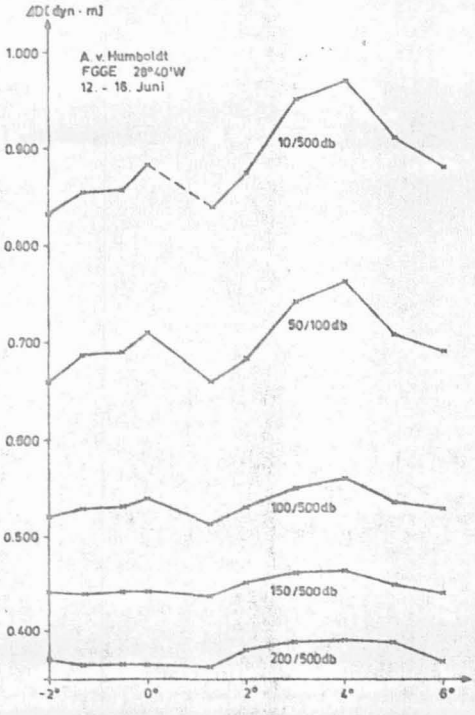
ΔD [dyn · m]
1.000
0.900
0.800
0.700
0.600
0.500
0.400
A. v. Humboldt
FGGE 28°40'W
12. - 16. Juni
10/500 db
50/100 db
100/500 db
150/500 db
200/500 db
-2°
0°
2°
4°
6°

Fig. 7

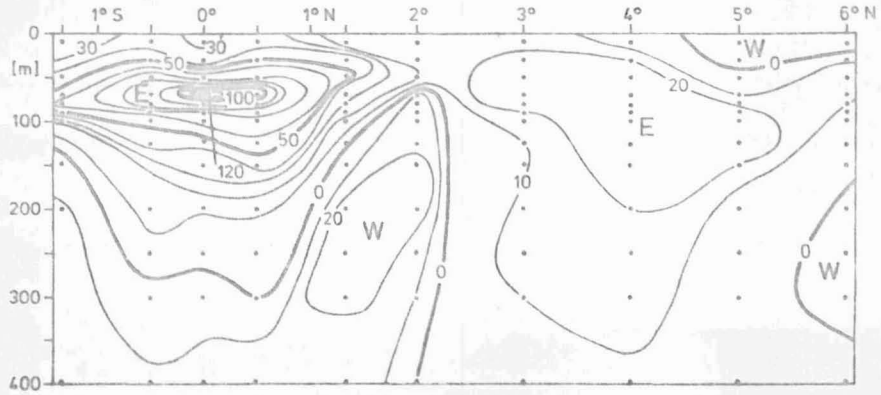


FGGE-FATE 79
u [cm·s$^{-1}$]
„Alexander v. Humboldt"
8.-12.5.1979

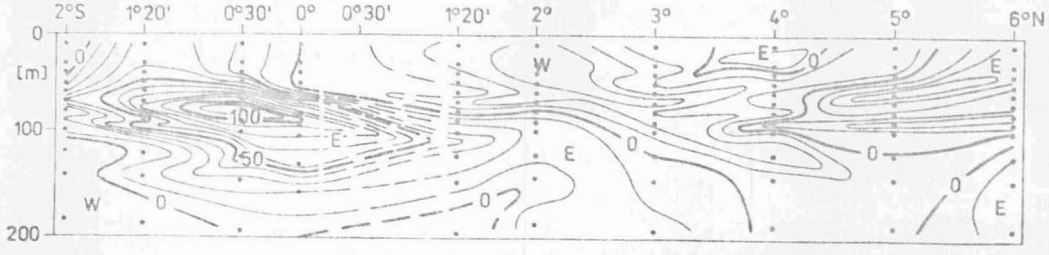


FGGE - FATE 79
u [cm s$^{-1}$]
„Alexander v. Humboldt"
12. - 17.6.79

Fig. 8

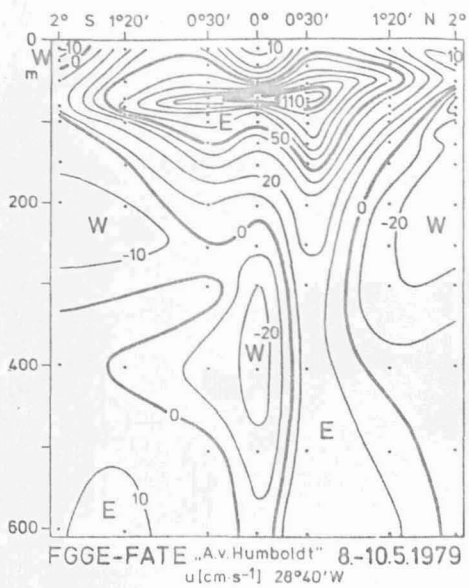


FGGE-FATE „A.v.Humboldt" 8.-10.5.1979
u[cm·s⁻¹] 28°40'W

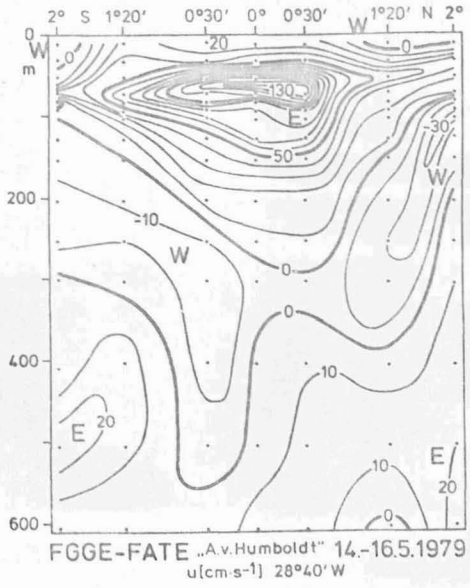


FGGE-FATE „A.v.Humboldt" 14.-16.5.1979
u[cm·s⁻¹] 28°40'W

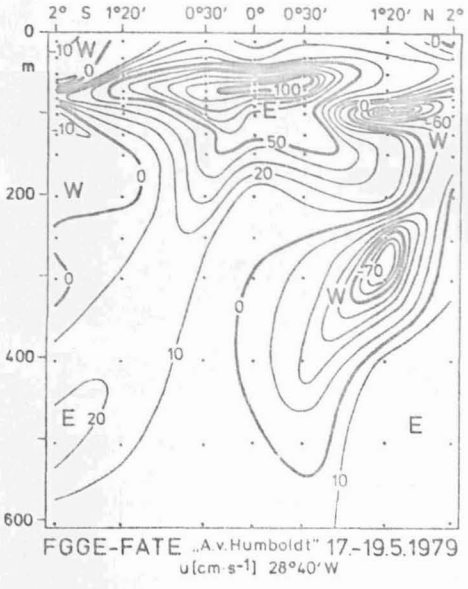


FGGE-FATE „A.v.Humboldt" 17.-19.5.1979
u[cm·s⁻¹] 28°40'W

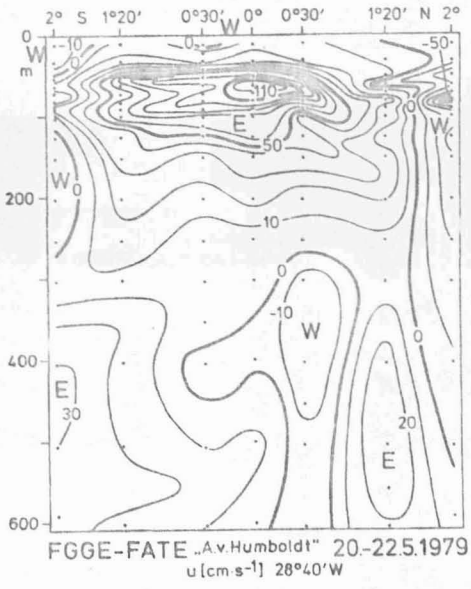


FGGE-FATE „A.v.Humboldt" 20.-22.5.1979
u[cm·s⁻¹] 28°40'W

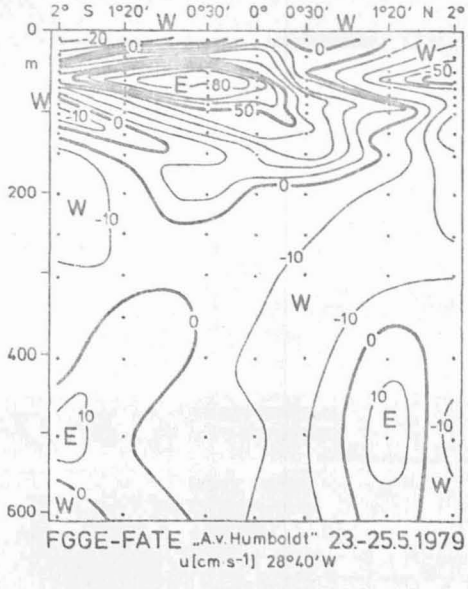


FGGE-FATE „A.v.Humboldt" 23.-25.5.1979
u[cm·s⁻¹] 28°40'W

Fig. 9

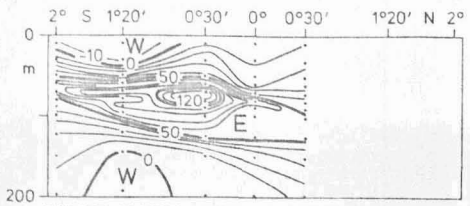


FGGE-FATE „A.v.Humboldt" 26.-27.5.1979
u[cm·s-1] 28°40'W

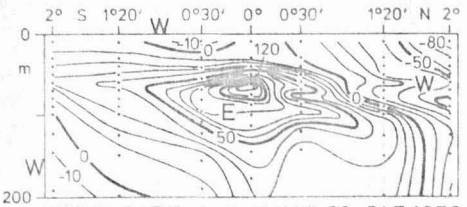


FGGE-FATE „A.v.Humboldt" 28.-31.5.1979
u[cm·s-1] 28°40'W

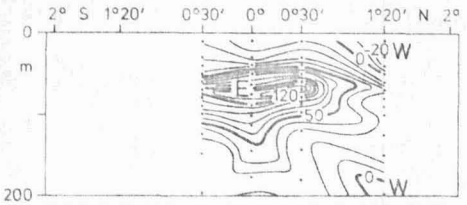


FGGE-FATE „A.v.Humboldt" 1.-2.6.1979
u[cm·s-1] 28°40'W

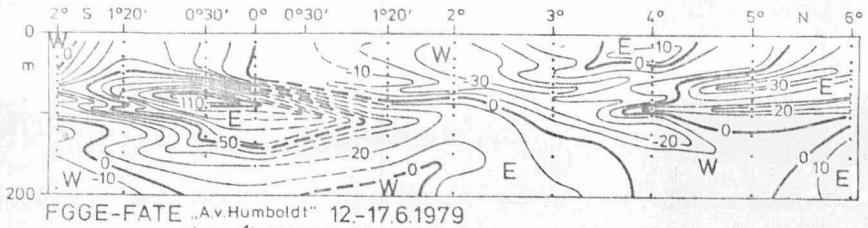


FGGE-FATE „A.v.Humboldt" 12.-17.6.1979
u[cm·s-1] 28°40'W

Fig. 10

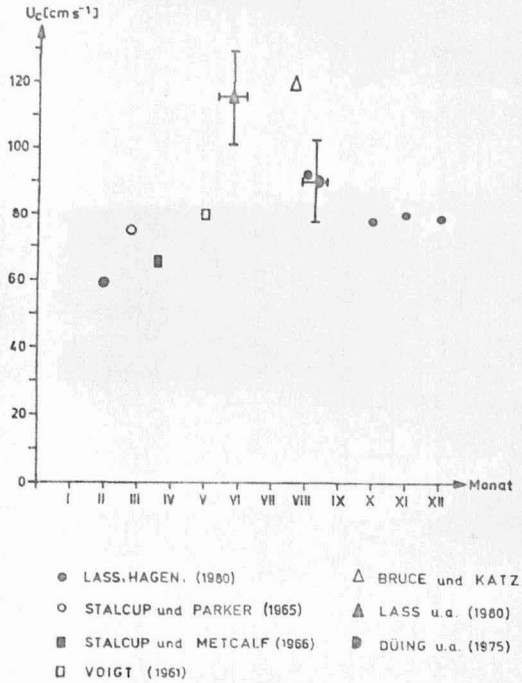


Fig. 11

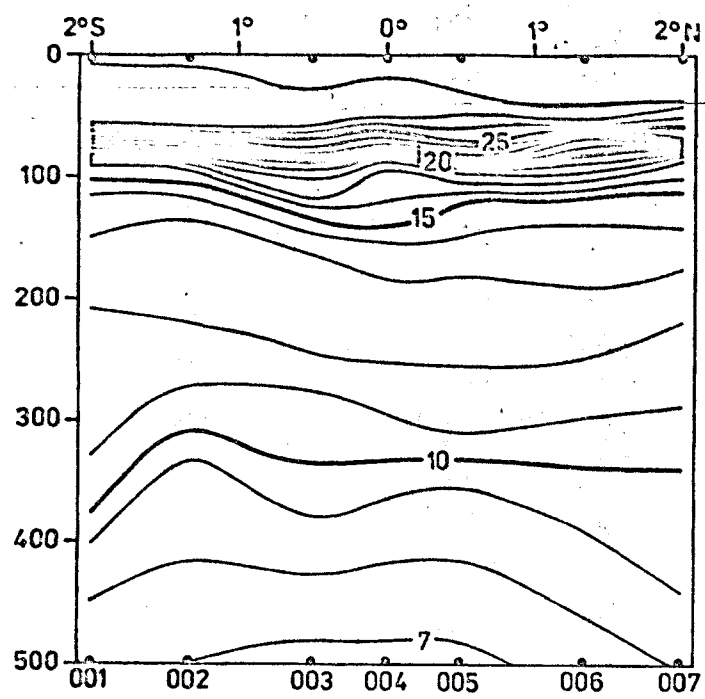


FGGE - FATE 79
„A.v.Humboldt"
28°40'W
T [°C]
14.-16.5.1979

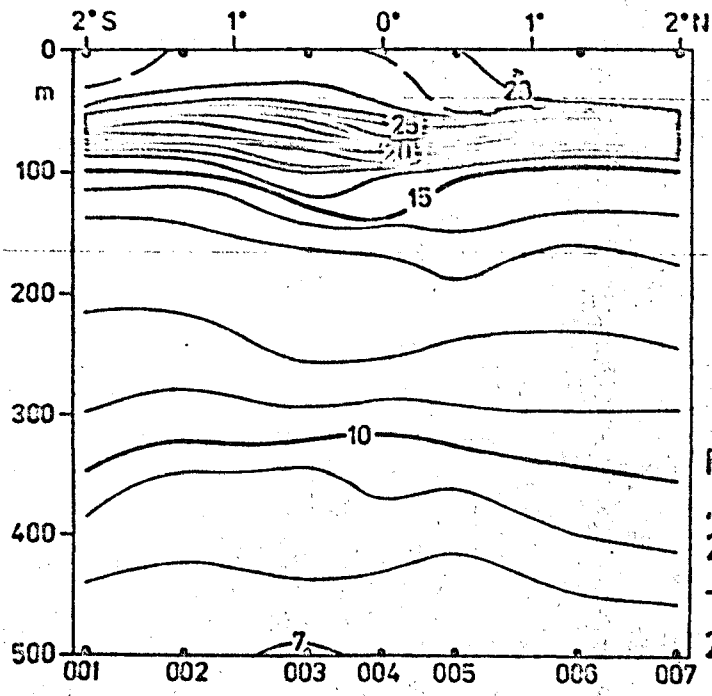


FGGE - FATE 79
„A.v.Humboldt"
28°40'W
T [°C]
23.-25.5.1979

Fig. 12

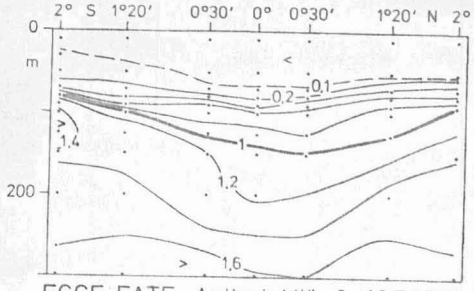


FGGE-FATE „A.v.Humboldt" 8.-10.5.1979
$PO_4$-P [µg-at./l] 28°40' W

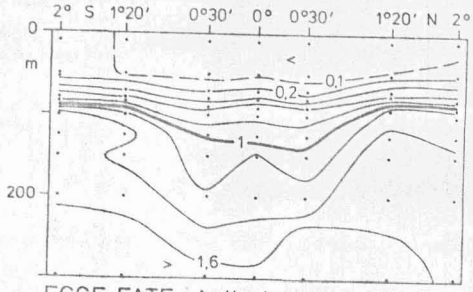


FGGE-FATE „A.v.Humboldt" 14.-16.5.1979
$PO_4$-P [µg-at./l] 28°40' W

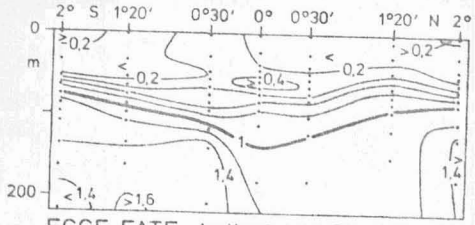


FGGE-FATE „A.v.Humboldt" 29.-30.5.1979
$PO_4$-P [µg-at./l] 28°40' W

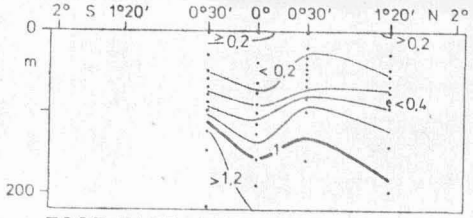


FGGE-FATE „A.v.Humboldt" 1.-2.6.1979
$PO_4$-P [µg-at./l] 28°40' W

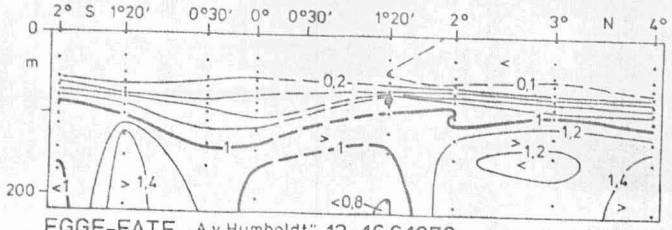


FGGE-FATE „A.v.Humboldt" 12.-16.6.1979
$PO_4$-P [µg-at./l] 28°40' W

Fig. 13

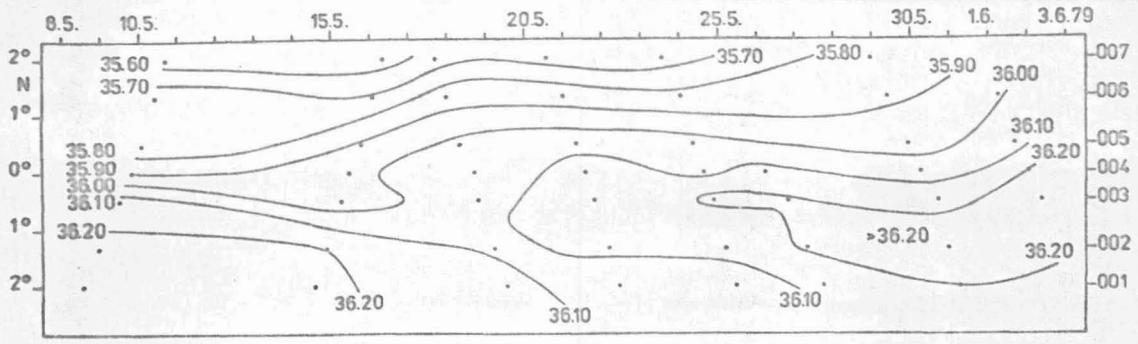


FGGE - FATE 79 S [‰]
„A.v.Humboldt" 10 m
28° 40' W

Fig. 14

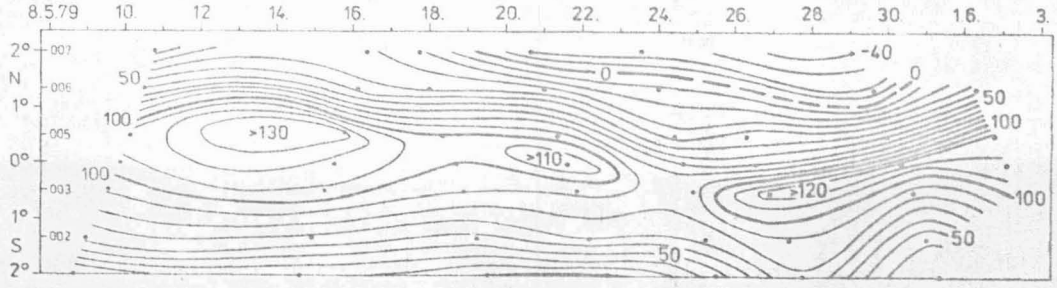


FGGE-FATE 79
$u_{max}$ [cm s$^{-1}$]
„Alexander v. Humboldt"
28° 40'W

Fig. 15